



This is a repository copy of *Non-axisymmetric instabilities in discs with imposed zonal flows*.

White Rose Research Online URL for this paper:
<http://eprints.whiterose.ac.uk/116132/>

Version: Supplemental Material

Article:

Vanon, R and Ogilvie, GI (2016) Non-axisymmetric instabilities in discs with imposed zonal flows. *Monthly Notices of the Royal Astronomical Society*, 463 (4). pp. 3725-3736. ISSN 0035-8711

<https://doi.org/10.1093/mnras/stw2238>

Reuse

Items deposited in White Rose Research Online are protected by copyright, with all rights reserved unless indicated otherwise. They may be downloaded and/or printed for private study, or other acts as permitted by national copyright laws. The publisher or other rights holders may allow further reproduction and re-use of the full text version. This is indicated by the licence information on the White Rose Research Online record for the item.

Takedown

If you consider content in White Rose Research Online to be in breach of UK law, please notify us by emailing eprints@whiterose.ac.uk including the URL of the record and the reason for the withdrawal request.



eprints@whiterose.ac.uk
<https://eprints.whiterose.ac.uk/>

Erratum: Non-axisymmetric instabilities in discs with imposed zonal flows

by R. Vanon^{*} and G. I. Ogilvie

Department of Applied Mathematics and Theoretical Physics, University of Cambridge, Centre for Mathematical Sciences, Wilberforce Road, Cambridge CB3 0WA, UK

Key words: errata, addenda – accretion, accretion discs – hydrodynamics – instabilities – turbulence.

This is an erratum to the paper ‘Non-axisymmetric instabilities in discs with imposed zonal flows’, which was published in MNRAS, 463(4), 3725 (2016).

First, a typo was seen in the divergence term of equation (23); this however has no effect on the results. Also, an error was found in the derivation of the adiabatic pressure terms in equations (24)–(26). The correct form of said equations is:

$$d_t \tilde{h}'_n = -\frac{k_y}{2} A_v (\tilde{h}'_{n-1} - \tilde{h}'_{n+1}) + \frac{A_h k}{2i} (\tilde{u}'_{n-1} - \tilde{u}'_{n+1}) - i(k_{xn} \tilde{u}'_n + k_y \tilde{v}'_n) \quad (1)$$

$$d_t \tilde{u}'_n = -\frac{A_v k_y}{2} (\tilde{u}'_{n-1} - \tilde{u}'_{n+1}) + 2\Omega \tilde{v}'_n - ik_{xn} \left(\frac{v_s^2}{\gamma} - 2 \frac{v_s \kappa}{|k_n| Q} \right) \tilde{h}'_n - (\gamma - 1) \left[\frac{ie_0 A_e}{2} (k_{x,n-1} \tilde{h}'_{n-1} + k_{x,n+1} \tilde{h}'_{n+1}) - \frac{k A_h}{2i} (\tilde{z}'_{n-1} - \tilde{z}'_{n+1}) + ik_{xn} \tilde{z}'_n \right] \quad (2)$$

$$d_t \tilde{v}'_n = -\frac{A_v}{2} [k (\tilde{u}'_{n-1} + \tilde{u}'_{n+1}) + k_y (\tilde{v}'_{n-1} - \tilde{v}'_{n+1})] - (2 - q)\Omega \tilde{u}'_n - ik_y \left(\frac{v_s^2}{\gamma} - 2 \frac{v_s \kappa}{|k_n| Q} \right) \tilde{h}'_n - (\gamma - 1) \left[\frac{ie_0 A_e}{2} k_y (\tilde{h}'_{n-1} + \tilde{h}'_{n+1}) + ik_y \tilde{z}'_n \right] \quad (3)$$

$$d_t \tilde{z}'_n = \frac{ke_0 A_e}{2i} (\tilde{u}'_{n-1} - \tilde{u}'_{n+1}) - \frac{A_v k_y}{2} (\tilde{z}'_{n-1} - \tilde{z}'_{n+1}) - i(\gamma - 1)e_0 \left\{ (k_{xn} \tilde{u}'_n + k_y \tilde{v}'_n) + \frac{A_e}{2} [k_{x,n-1} \tilde{u}'_{n-1} + k_{x,n+1} \tilde{u}'_{n+1} + k_y (\tilde{v}'_{n-1} + \tilde{v}'_{n+1})] \right\}, \quad (4)$$

where $k_n = \sqrt{k_{xn}^2 + k_y^2}$ and $k_{x,n \pm 1} = k_{x0} + (n \pm 1)k + q\Omega k_y t$.

Since the corrections of equations (2)–(4) only affect terms involving e , the results for the isothermal case (Section 3, Figs 2–9 and Figs A1–A3) are unaffected. Fig. 10, which represented a comparison to the isothermal case of Fig. 6 using $\gamma = 1.5$, also appears largely unaffected by the correction. On the other hand, the correction has repercussions on Figs 11–13 of the original paper. The corrected version of these figures is proposed here in Figs 1–3.

Fig. 1 shows the growth rate contours in the presence of an axisymmetric structure in the entropy only (i.e. there is no structure in the potential vorticity ζ), with $\gamma = 5/3$, $A_s = 0.25$ and $k_v s / \Omega =$

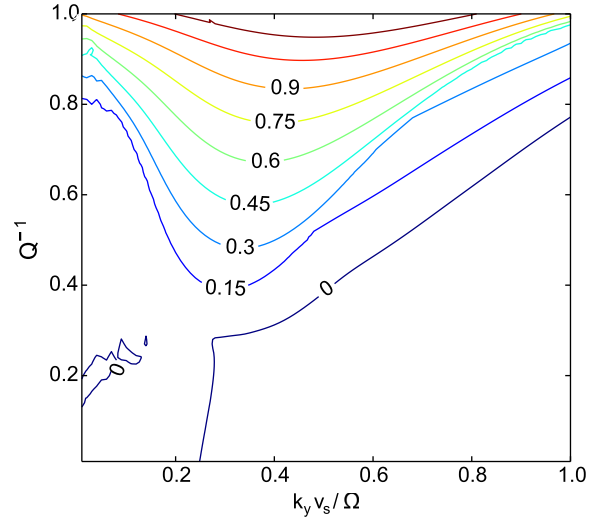


Figure 1. Growth rate contours for $k_v s / \Omega = 2$, $\gamma = 5/3$, $A_\zeta = 0$ and $A_s = 0.25$ showing the gravitationally-induced instability having spread to low values of Q^{-1} and an instability being present for $Q^{-1} = 0$, too.

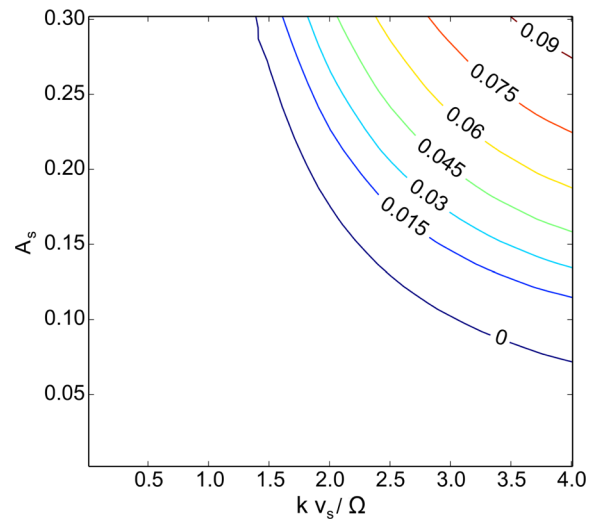


Figure 2. Contours of the growth rate (in units of Ω) maximized with respect to k_y in the $k_v s / \Omega - A_s$ plane for $A_\zeta = 0$, for non-SG conditions. As in the isothermal case again the growth rate strength increases with increasing $k_v s / \Omega$ and A_s , although no instability is detected for $A_s \lesssim 0.075$ or $k_v s / \Omega \lesssim 1.5$ in the chosen range. In this case the growth rates achieved are roughly 1 order of magnitude smaller than in the isothermal case. The flow is in this case Rayleigh stable for all parameter values.

* E-mail: rv288@cam.ac.uk

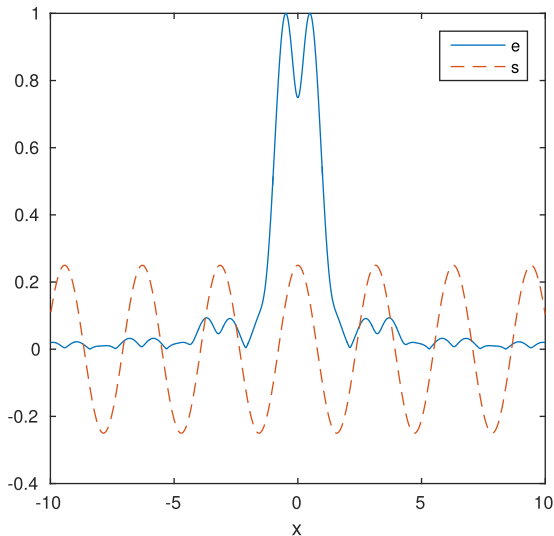


Figure 3. Real space visualization of the normalized internal energy e (full, blue line) associated with the instability detected for non-SG conditions, for $k_y v_s / \Omega = 0.075$, $k v_s / \Omega = 2$, $A_s = 0.25$, $A_\zeta = 0$ and $\gamma = 5/3$. The entropy perturbation is also shown (dashed, red line) to show that this type of instability is localised around a maximum in s .

2 (instead of $k v_s / \Omega = 6$ as in the original paper’s Fig. 11). The qualitative behaviour of the instability is very similar to that of the original paper’s Fig. 11: the Kelvin-Helmholtz instability is not triggered due to the absence of a structure in ζ , while the present gravitational instability progressively reaches weaker self-gravitating (SG) conditions as the value of A_s is increased. This again occurs until eventually the non-self-gravitating case ($Q^{-1} = 0$) becomes weakly unstable, as shown in Fig. 1. Also similarly to the original paper’s figure, it remains unclear whether the $Q^{-1} \neq 0$ and $Q^{-1} = 0$ instabilities are of the same nature.

Fig. 2 represents the k_y -maximized growth rates of the instability detected at $Q^{-1} = 0$ in Fig. 1 as a function of the zonal flow’s amplitude and wavenumber. Once again, the results are qualitatively similar to those presented in the original paper, with increasing zonal flow amplitude and wavenumber yielding a stronger instability. In this case however, the instability is triggered for a wider range of parameters, which is however slightly more restricted compared to that of the Kelvin-Helmholtz instability in the isothermal regime. Furthermore, the growth rate of the instability is roughly 3 orders of magnitude larger compared to the original paper’s Fig. 12, but still weaker than the isothermal Kelvin-Helmholtz instability (by about 1 order of magnitude).

Lastly, the internal energy e associated with the non-SG instability in Fig. 1 is visualized in Fig. 3 using the Poisson summation formula method. This shows the energy as a function of x for $k_y v_s / \Omega = 0.075$, $A_s = 0.25$, $A_\zeta = 0$ and $\gamma = 5/3$. The results are qualitatively similar to the figure in the original paper (Fig. 13), with the energy (blue, full line) being well localised around an entropy maximum (red, dashed); the energy peak at $x = 0$ is however wider due to the smaller wavenumber used in Fig. 1 ($k v_s / \Omega = 2$) compared to the one used in the respective figure in the original paper ($k v_s / \Omega = 6$).

The correction does not alter the conclusions reached by the original paper. As mentioned previously, the isothermal scenario (on which the paper is primarily focused) is completely unaffected and the original results stand true. While the adiabatic instability with $A_\zeta = 0$ is affected by the correction, its qualitative behaviour remains largely unchanged; it is simply observed to be stronger than originally thought, and to be triggered for a larger set of A_s and $k v_s / \Omega$ values.

We thank Antoine Riols for bringing the error to our attention. The preprint on arXiv has been suitably updated.

This paper has been typeset from a \LaTeX file prepared by the author.